

CHARACTERIZATION OF NITROGEN-RICH SILICON NITRIDE FILMS GROWN BY THE ELECTRON CYCLOTRON RESONANCE PLASMA TECHNIQUE

L. Wang¹, H. S. Reehal¹, F. L. Martínez², E. San Andrés³, and A. del Prado³.

¹ *Faculty of Engineering, Science, and Technology, South Bank University, 103 Borough Road, London SE1 0AA, United Kingdom.*

² *Departamento de Electrónica y Tecnología de Computadoras, Universidad Politécnica de Cartagena, 30202 Cartagena, Spain.*

³ *Departamento de Física Aplicada III, Universidad Complutense de Madrid, 28040 Madrid, Spain.*

Short title: “Characterization of silicon nitride films grown by electron cyclotron resonance”.

Classification numbers (PACS): 61.43.Er, 68.55.Ln, 77.84.Bw, 78.30.Ly, 81.15.Gh, 82.80.Yc

ABSTRACT

Amorphous hydrogenated silicon nitride films have been deposited by the electron cyclotron resonance plasma technique, using N₂ and SiH₄ as precursor gases. The gas flow ratio, deposition temperature and microwave power have been varied in order to study their effect on the properties of the films, which were characterized by Rutherford back-scattering spectrometry, elastic recoil detection analysis (ERDA), Fourier transform infrared spectroscopy, and ellipsometry. All samples show N/Si ratios near or above the stoichiometric value (N/Si=1.33). The hydrogen content determined from ERDA measurements is significantly higher than the amount detected by infrared spectroscopy, evidencing the presence of non bonded H.

As the N₂/SiH₄ gas flow ratio is increased (by decreasing the SiH₄ partial pressure), the Si content decreases and the N-H concentration increases, while the N content remains constant, resulting in an increase of the N/Si ratio. The decrease of the Si content causes a decrease of the refractive index and the density of the film, while the growth ratio also decreases due to the limiting factor of the SiH₄ partial pressure. The infrared Si-N stretching band shifts to higher wavenumbers as the N-H concentration increases.

The increase of deposition temperature promotes the release of H, resulting in a higher incorporation of N and Si into the film and a decrease of the N/Si ratio. The effect of increasing the microwave power is analogous to increasing the N₂/SiH₄ ratio, due to the increase in the proportion of nitrogen activated species.

I INTRODUCTION

Silicon nitride ($\text{SiN}_x\text{:H}$) is an extensively used dielectric in both silicon and III-V semiconductor device technologies. The most usual applications include passivation layers [1, 2], optoelectronic devices [3, 4], thin film transistors (TFTs) [5, 6], and metal-insulator-semiconductor (MIS) devices [7, 8]. Plasma deposited silicon nitride has also emerged as a passivating material for crystalline silicon solar cells, which simultaneously provides good antireflection properties [9, 10].

Electron cyclotron resonance plasma enhanced chemical vapor deposition (ECR-PECVD) is a well established technique for the deposition of $\text{SiN}_x\text{:H}$ films. As other plasma techniques, it allows low deposition temperatures, satisfying the requirements of ultra large scale integration technology (ULSI) [11, 12]. Additionally, substrates are placed outside the plasma region, reducing the damage produced by ion bombardment [13]. Finally, the ECR technique is a very efficient method for the activation of the precursor gases [14, 15], obtaining high density plasmas and making possible the use of N_2 instead of NH_3 , thereby reducing the H content of the films.

There is extensive research devoted to the analysis of the properties of amorphous hydrogenated silicon nitride films deposited by ECR [16, 17, 18, 19, 20]. Films with N/Si ratios greater than 1.33 show good interface properties when used in silicon based MIS devices [18, 21]. Additionally, nitrogen-rich films have been found to passivate the phosphorus vacancies in InP based MIS structures, allowing good interface properties without the deposition of an interface control layer [22, 23, 24].

In this paper, the influence of gas flow ratio, deposition temperature and microwave power on the properties of ECR deposited N-rich $\text{SiN}_x\text{:H}$ films will be analyzed in detail. The films have been characterized by Rutherford back-scattering spectrometry (RBS), elastic recoil detection analysis (ERDA), Fourier transform infrared spectroscopy (FTIR) and ellipsometric analysis. The combination of the composition measurements (RBS and ERDA) with the information on the bonding structure derived from FTIR spectroscopy has allowed a detailed study on the incorporation of H to the films and its effects on the composition, density and structural properties.

II EXPERIMENT

The $\text{SiN}_x\text{:H}$ films have been obtained by ECR-PECVD. The load-locked deposition system (Plasma Technology AMR) has been described previously [25]. It is of stainless steel construction and pumped with a 1000 l/s Leybold turbomolecular pump, capable of reaching

base pressures of about 10^{-7} Torr. The process chamber was equipped with a retractable Langmuir probe (HIDEN Analytical) which could be positioned in the vicinity of the substrate for plasma monitoring. Electronic grade nitrogen and silane were introduced into the ECR plasma chamber and the process chamber, respectively, the latter through a gas distribution ring.

Polished p-type silicon wafers (resistivity about $1 \Omega\text{cm}$) were used as substrates. Before film growth, these substrates were subjected to standard RCA cleaning, dipped in 10:1 diluted HF solution and blown dry using nitrogen. Different sample series were deposited with a constant N_2 gas flow of 50 sccm and a SiH_4 flow ranging between 2 and 5 sccm, so that the N_2/SiH_4 gas flow ratio varied from 10 to 25. Deposition temperature was varied from 230 °C to 500 °C, while microwave power was in the range between 200 W and 500 W. Pressure was kept constant at about 3.5 mTorr. Table 1 shows the deposition conditions for the most representative samples.

The refractive index and thickness of the films were determined by a PLASMOS SD2100 ellipsometer at an incidence angle of 70° and a wavelength of 633 nm. A J.A.Woollam Company M-88 ellipsometer was also used at angles of incidence between 65° to 75° to measure the wavelength dependence of the refractive index over the spectral range 280-760 nm. The refractive index of the film was modeled using the Cauchy dispersion equation [26]. The hydrogen, silicon, and nitrogen content were measured by RBS and ERDA, using 1.5 MeV He^+ ions at 160° scattering angle for RBS and 26° for ERDA. The measurements were carried out at Surrey University (UK) and the WinNDF code based on simulated annealing [27] was used for data analysis. Absolute RBS errors can be estimated as $\pm 5\%$, while ERDA errors are $\pm 10\%$.

FTIR spectroscopy was performed using a Nicolet Magna-IR 750 series II spectrometer. The spectra were measured in the transmission mode at normal incidence. Bonded hydrogen content was determined from the Si-H and N-H stretching bands according to the well known method developed by Lanford and Rand [28]. The error of these bond concentrations is difficult to estimate, because it depends not only on the calibration factors and sample thickness, but also on the subjective error introduced by the experimenter during the process of baseline correction prior to the calculation of the band areas. Overall it can be estimated to be $\pm 10\%$.

III RESULTS

A. Growth rate

Growth rate was determined from the thickness of the films obtained by ellipsometry. Figure 1 shows the growth rate as a function of deposition temperature (T_d) for samples deposited at 500 W and $N_2/SiH_4=12.5$. The growth rate remains roughly constant for T_d up to about 300 °C and then it increases, with a steep raise for $T_d=500$ °C. Concerning the influence of the gas flow ratio, a decrease of the growth rate when decreasing the SiH_4 partial pressure was observed. This is the expected behavior, as silane is the precursor gas which limits the reaction [29, 30].

B. RBS/ERDA

The hydrogen, nitrogen and silicon atomic concentrations measured by RBS and ERDA are shown in Table 1. The concentrations were obtained by normalizing the RBS or ERDA atom/cm² count to the thickness of the films. The atomic per cent content of each species was calculated normalizing the total H, Si, and N content to 100%. A 10% relative error is estimated for these results.

Most samples show a N/Si ratio higher than the stoichiometric value, so that N-rich films were obtained. By stoichiometric films we mean $N/Si=1.33$, although actual stoichiometric films should have no H content. In the same way, we call N-rich those samples with a N/Si ratio greater than 1.33, even if due to the H content the N atomic percent is lower than in pure stoichiometric Si_3N_4 films. N/Si ratios below 1.33 were obtained for samples deposited at high silane partial pressure and high temperature, though the 1.33 value fits within the error margin for all samples.

Concerning the influence of the different deposition parameters, the following broad trends are observed. As the silane partial pressure during deposition is increased, the silicon content increases, while the N content remains roughly constant and the H content decreases, so that the N/Si ratio decreases. When increasing T_d , both the N and Si content increase, while the H content significantly decreases. If density calculations are performed from the concentrations of the different species, an increase of the density of the film is observed when increasing T_d . Additionally, the N/Si ratio is lower for the higher values of T_d , so that the incorporation of Si is enhanced with respect to the incorporation of N when T_d is increased.

C. FTIR Spectroscopy

The FTIR spectrum of the samples is dominated by the Si-N stretching band, with its maximum located between 840 and 860 cm^{-1} depending on the deposition conditions. The N-H stretching band is also present, as well as a very weak Si-H stretching band. The concentrations of N-H and Si-H bonds are shown in Table 1. It must be noted that the Si-H results must be handled with care, as the concentration is very low and close to the detection limit. However, the trends are very clear.

In all samples the N-H bond concentration is about one order of magnitude higher than the Si-H one. This result is perfectly consistent with the N/Si ratios above 1.33 obtained by RBS.

The maximum value of the total bonded hydrogen content is about $1 \times 10^{22} \text{ cm}^{-3}$ and it is obtained for the samples deposited at the lowest temperature and highest N_2/SiH_4 ratio (lowest SiH_4 flow). The low value of bonded hydrogen is characteristic of ECR deposited $\text{SiN}_x\text{:H}$ using N_2 as precursor gas for nitrogen instead of NH_3 [31, 32]. It must be noted, however, that the H content obtained by ERDA is significantly higher than the FTIR results, as shown in Table 1. FTIR spectroscopy detects only H present in the form of N-H or Si-H bonds, while ERDA detects both the bonded and non-bonded H. So we conclude there is a significant amount of non-bonded H in the samples. Evidence of the presence of non-bonded H in $\text{SiN}_x\text{:H}$ films has already been reported and is known to play an important role in structural relaxation processes [33, 34]. Figure 2 shows the non-bonded hydrogen content obtained by subtracting the total bonded H content calculated by FTIR spectroscopy from the total hydrogen detected by ERDA. Lower non-bonded H values are obtained for higher deposition temperatures.

Regarding the bonded hydrogen content, Figure 3 shows the N-H and Si-H bond concentrations as a function of the N_2/SiH_4 ratio for two series deposited at different substrate temperatures. The two types of bonds follow opposite trends. While the N-H bond concentration increases for higher values of the N_2/SiH_4 gas flow ratio and decreases for higher deposition temperatures, the Si-H concentration decreases in the first case and increases in the second. As the total bonded H content is mainly due to N-H bonds, it follows their same trend.

As the N_2/SiH_4 ratio increases, a shift (up to about 13 cm^{-1}) of the Si-N band to higher wavenumbers is observed, coincident with the increase of the N-H bond concentration. Figure 4 shows the trends for the wavenumber of the Si-N stretching band. When the deposition temperature is increased, a shift of the Si-N band to lower wavenumbers is observed, again in

coincidence with the trend of the N-H bond density. The Si-N band also gets narrower for higher temperatures, as shown in Figure 5 by the full width at half maximum (FWHM) parameter.

The effect of increasing the microwave power during deposition is very similar to increasing the N_2/SiH_4 ratio: the Si-N band slightly shifts to higher wavenumbers, the N-H concentration increases and the Si-H concentration decreases.

D. Refractive index

The relation between the refractive index (measured at 633 nm) and the N_2/SiH_4 ratio is shown in Figure 6 for samples deposited at 400 W and $T_d=310$ °C. A decrease from 1.94 to 1.88 is observed when N_2/SiH_4 increases from 10 to 25 (corresponding to a decrease of the SiH_4 flow from 5 sccm to 2 sccm). Figure 7 shows the refractive index versus wavelength for samples deposited at 500 W, $N_2/SiH_4=12.5$ and different deposition temperatures. An increase to higher values of the refractive index is observed when increasing T_d .

IV DISCUSSION

A. Influence of the gas flow ratio

The main reaction during the deposition of $SiN_x:H$ is the formation of Si-N bonds from the plasma activated N_2^* species which react with the SiH_4 molecules. It can be assumed that no N-N bonds are formed due to their low binding energy $E(N-N) = 1.65$ eV with respect to other bonds actually present in the films: $E(Si-N) = 3.45$ eV, $E(N-H) = 4.05$ eV, $E(Si-H) = 3.34$ eV and $E(Si-Si) = 2.3$ eV [35]. Si-Si bonds, despite their relatively low binding energy (but higher than that of N-N bonds), are known to play an important role in the properties of $SiN_x:H$ films [36]. Additionally, hydrogen is incorporated in the form of Si-H and N-H bonds, as well as in atomic or molecular form in microvoids of the structure.

It is well known that the composition of the films is strongly dependent on the deposition conditions. When low N_2/SiH_4 ratios or low values of microwave power are used silicon-rich films are obtained, as the SiH_4 species produce Si-Si and Si-H bonds in the growing film [37]. On the contrary, when the N_2/SiH_4 ratio or the microwave power are increased, stoichiometric or nitrogen-rich $SiN_x:H$ films can be obtained. Silicon-rich films usually have a higher concentration of Si-H bonds than N-H bonds, while nitrogen-rich films show the opposite behavior [38, 39].

It is usually found that, for a given N_2/SiH_4 ratio, there is a threshold value of the microwave power for which there are enough N_2^* activated species to react with the activated

SiH₄ to exhaustion. In an analogous way, for a given microwave power, there is a threshold value of the N₂/SiH₄ ratio for which the same result is obtained [40]. Once this threshold value has been reached, near stoichiometric SiN_x:H films are obtained, while Si-Si and Si-H bonds tend to disappear. Further increase of the microwave power or the N₂/SiH₄ ratio enhances the incorporation of N to the films, mainly in the form of N-H bonds [38, 39].

In this work, all samples show a concentration of N-H bonds significantly higher than the Si-H concentration, suggesting the films are N-rich. This conclusion is supported by the RBS measurements of the N and Si concentrations, which give N/Si ratios above 1.33 for all samples within the error margin.

Additionally, the growth rate significantly decreases when increasing the N₂/SiH₄ ratio (that is, when decreasing the SiH₄ partial pressure). This same result has been widely reported [29, 30, 41] and is explained as follows. For high N₂/SiH₄ gas flow ratios, such as those used in this work, there is an excess of N₂^{*} activated species, so that deposition rate is controlled by the arrival of silane species at the surface of the film. In this work, the increase of the N₂/SiH₄ ratio means a decrease of the amount of SiH₄ during deposition, and therefore a reduction of the number of Si-related species. Hence the reaction is inhibited and the growth rate decreases. This result is supported by Langmuir probe measurements carried out above the growing film. Figure 8 shows the total ion density measured for different N₂/SiH₄ ratios. This parameter behaves in an opposite way to the growth rate. Optical emission spectroscopy measurements have shown that N₂⁺ ions are the predominant species in the downstream region of an ECR N₂ plasma [42, 43]. This is likely to be the case in the present work. As total N₂ flow is constant, the increase of the N₂/SiH₄ ratio means a lower number of silane species to react with. So, a lower proportion of N₂⁺ ions can react, the ion density increases and the reaction rate decreases. (Note that the data of Figure 8 were recorded using non-optimized settings for the magnet currents. Using the optimized settings employed during film growth resulted in an order of magnitude increase in the ion density, with the same trend as shown in this figure).

The behavior of the growth rate is perfectly consistent with the conclusion that N-rich films have been obtained. However, even if there is an excess of N₂^{*} species to react with the activated SiH₄ molecules until exhaustion, there is still a small amount of Si-H bonds, which suggests that the reaction mechanisms of SiH₄ to produce Si-Si and Si-H bonds are still present, although in a very low proportion.

Composition of the films is also affected by the N₂/SiH₄ ratio. As this parameter increases, both the Si content and Si-H concentration decrease, while the N content remains

constant and the N-H concentration increases. There are two mechanisms for the incorporation of N to the films by the formation of either Si-N or N-H bonds, the former being the predominant reaction. As the N_2/SiH_4 ratio is increased, it is expected that an enhancement of the incorporation of N with respect to the incorporation of Si occurs in the film, so that a higher N/Si ratio is obtained. Once the stoichiometric value $N/Si=1.33$ has been reached, this parameter can increase by three different mechanisms: the substitution of Si-H bonds by Si-N bonds, the substitution of Si-Si bonds by Si-N bonds, and the substitution of Si-N bonds by N-H bonds. The first mechanism must be present, as the Si-H bond concentration decreases (Figure 3). However, this mechanism is not very significant, as the Si-H concentration is very low. The same conclusion can be extended to the Si-Si bonds, which must be in very low proportion if they are present at all in the film. Additionally, any of these mechanisms should result in an increase of the N content, rather than the observed decrease of the Si content. Figure 3, shows the increase of the N-H bond concentration as the N_2/SiH_4 ratio increases, which suggests that the results are explained by the formation of N-H bonds at the expense of Si-N bonds, so that the N content remains constant while the Si content decreases and the N-H concentration increases.

It is important to note that the increase of the N/Si ratio observed when increasing the N_2/SiH_4 ratio is not due to an increase of the N content, but a decrease of the Si content. This result supports the conclusion that the reaction for the formation of Si-N bonds is saturated. However, a different mechanism for the incorporation of N to the film is the formation of N-H bonds. In this work, the N_2/SiH_4 ratio is increased by decreasing the SiH_4 gas flow. So, while the number of activated N_2^* species remains constant, the number of activated Si related species decreases, resulting in a lower reaction rate and an increase of the concentration of excess N_2^* species. This excess N_2^* enhances the reaction to form N-H bonds, so that the overall result is a film with a higher N-H concentration and a lower Si content, while the N content remains constant. It is concluded that even for N-rich samples, a relative increase of N_2^* activated species with respect to the Si related ones has an influence on composition due to the formation of N-H bonds.

Figure 4 shows the shift of the Si-N stretching band to higher wavenumbers as the N_2/SiH_4 ratio increases. This shift is related to the increase of the N-H concentration. A similar behavior has already been reported and attributed to the different electronegativities of H and Si. The presence of a H atom bonded to a N site, in place of a Si atom, results in a decrease in the length of neighboring Si-N bonds and, therefore, an increase in the oscillating frequency [44, 45].

Figure 9 shows the wavenumber of the Si-N stretching band as a function of the N-H concentration for samples deposited at different conditions (gas flow ratio, temperature and microwave power). This same trend has been reported by other authors [44, 46], although for the same values of N-H concentration higher values of the Si-N wavenumber are obtained in this work. In addition to the influence of the N-H concentration, the exact location of this band also depends on other characteristics of the films such as the Si-Si and Si-H concentration or the stress. The trend observed in Figure 9 suggests that the shift of the Si-N band to higher wavenumbers is related directly to the increase of the N-H concentration rather than to a direct effect of the changing of the N/Si ratio of the film when increasing the N_2/SiH_4 ratio.

The decrease of the refractive index when increasing the N_2/SiH_4 ratio, shown in Figure 6, is explained by the decrease in the Si content of the film. It has been reported that a change in the refractive index value from 2.3 to 3.6 occurs for samples with composition varying from silicon nitride to amorphous silicon [41]. Films deposited using pure silane had a refractive index of 3.9, which corresponds to amorphous silicon [47]. As the N_2/SiH_4 ratio increases, less Si is being incorporated to the films, so that the refractive index decreases. Additionally, samples deposited at the highest N_2/SiH_4 ratios show a lower density, (calculated from the H, N, and Si concentration) than those deposited at the lowest N_2/SiH_4 ratios. This lower density may also be related to the lower refractive index values of those samples.

B. Influence of the deposition temperature.

The deposition temperature (T_d) has been found to strongly influence the properties of the films. The growth rate increases when increasing T_d , as shown in Figure 1. For low deposition temperatures, below 400 °C, there is no significant change in the growth rate. However, when T_d is raised up to 500 °C, there is a steep rise in the growth rate. This non linear behavior suggests a thermal activation process, with a threshold value around 500 °C. This temperature is high enough to result in a significant activation of SiH_4 at the surface of the growing film, resulting in an enhanced deposition rate.

Other authors have reported a decrease of the growth rate when increasing T_d for ECR deposited $SiN_x:H$ films, for similar deposition temperatures to those used in this work [29, 46, 48]. In these references the decrease of the growth rate is explained by the release of NH_x species, which is enhanced by the increase of T_d . A decrease of the N-H bond concentration when increasing T_d is indeed observed in our samples (Figure 3). So, a similar H release

mechanism may take place. However, it must be noted that the growth rate in this work (15-20 nm/min) is much higher than those reported in references [29], [46], and [48], which makes the release of NH_x species less likely, and the effect of this mechanism on the growth rate is less significant than the increase associated to the thermal process discussed above.

Concerning composition, when T_d is increased both the Si and N content increase while the H content decreases. Additionally, the N/Si ratio decreases. The increase of T_d activates the release of non-bonded H and the breaking of weak H bonds so that the H content decreases, and the relative amount of N and Si increases, resulting in a more dense film. Additionally, T_d enhances the incorporation of Si to the film with respect to the incorporation of N, as evidenced by the decrease of the N/Si ratio. This result is consistent with the SiH_4 activation process explained above, as a higher concentration of active Si species would result in a higher incorporation of Si to the film. However, the decrease of the N/Si ratio is observed even for the samples deposited at temperatures too low for the activation process to take place. Therefore, there must be an additional mechanism to explain this result.

As previously discussed in section A, N-H bonds are incorporated at the expense of Si atoms. Therefore, the decrease of the N-H bond concentration when increasing T_d results in a higher Si content, as Si-N bonds are formed instead of N-H bonds. So, the effect of increasing T_d is opposite to increasing the N_2/SiH_4 ratio.

The effect of T_d on the bonded hydrogen content is shown in Figure 3. The N-H concentration decreases, while the Si-H concentration increases. A similar behavior has been reported when $\text{SiN}_x\text{:H}$ films are annealed at temperatures below 500 °C [19]. In this temperature range, the following reaction takes place, resulting in an increase of the Si-H bond concentration and a decrease of the N-H one [49]:



However, the decrease observed for the N-H concentration is higher than the increase of the Si-H concentration. Additionally, the samples studied in this work show N/Si ratios above the stoichiometric value, with a very low concentration of Si-Si bonds. So, this reaction alone does not explain the results obtained in this work. The increase of the Si-H and the decrease of the N-H concentrations are related to the change in composition when increasing T_d , which has been discussed above. There is a substitution of N-H bonds with Si-N bonds which explains the decrease of the concentration of N-H bonds, while the enhanced incorporation of Si with respect to N results in an increase of the Si-H concentration. Additionally, the N-H bond concentration may decrease due to the release of NH_x volatile species when increasing T_d , as previously suggested.

As T_d is increased, a shift of the Si-N stretching band to lower wavenumbers is also observed (Figure 4). This shift is related to the decrease of the N-H bond concentration, as explained above.

Figure 5 shows the FWHM of the Si-N stretching band as a function of T_d . This parameter is related to the structural order of the film, with a higher value of FWHM meaning a higher disorder, as the dispersion of different bonding environments is higher [50]. As T_d is increased, a decrease in FWHM is observed indicating an improvement of the structural order and therefore an improvement of the quality of the films.

Finally, the refractive index increases when increasing T_d , as shown in Figure 7. This increase of the refractive index is related to the densification of the film and the change in composition, resulting in a higher Si content.

C. Influence of the microwave power.

The effect of increasing microwave power is very similar to increasing the N_2/SiH_4 ratio (decreasing the SiH_4 partial pressure). The final result is a relative increase in the concentration of N_2^* activated species. The behavior of the bonded H (increase of N-H and decrease of Si-H concentrations) and the Si-N stretching band (shift to higher wavenumbers) is the same as explained previously.

However, it is interesting to compare our results with those reported by other authors [48]. Hattangady *et al.* observe a decrease of the N-H bond concentration when increasing microwave power, while in this work, the N-H concentration increases. Such decrease of the N-H is explained by the formation of volatile NH_x species. It has been previously discussed that this reaction takes place for deposition rates significantly lower than those reported in this work.

V SUMMARY

The effect of deposition conditions has been analyzed in N-rich $SiN_x:H$ films. Gas flow ratio and microwave power values have been adjusted to produce an excess of N_2^* activated species to react with the active SiH_4 molecules to exhaustion, so that N-rich films have been obtained ($N/Si > 1.33$). Comparison between ERDA and FTIR measurements evidences the presence of a significant amount of non-bonded hydrogen.

The increase of the N_2/SiH_4 ratio results in an increase of the N/Si ratio above the stoichiometric value ($N/Si = 1.33$), while the N content remains constant. The increase of the N-H concentration and the decrease of the Si atomic percent provide evidence of a

substitution mechanism which leads to the formation of N-H bonds at the expense of Si-N bonds. The Si-H concentration also decreases when increasing the N_2/SiH_4 gas flow ratio. The same result is observed when increasing the microwave power. For a given deposition temperature, the composition of the film is determined by the proportion between the N_2^* activated species and the reactive SiH_4 molecules.

When the deposition temperature is increased, the H content significantly decreases and the incorporation of N and Si is enhanced, resulting in a densification of the film. Additionally, increasing T_d enhances the incorporation of Si with respect to N, obtaining lower N/Si ratios for higher deposition temperatures. This result is explained by the formation of Si-N bonds at the expense of N-H ones. Additionally, this change in composition results in an increase of the Si-H concentration. The increase of T_d also causes a significant increase of the growth rate for temperatures around 500 °C. This behavior is attributed to a thermal activation mechanism. The FWHM of the Si-N stretching band decreases when increasing T_d , evidencing an improvement of the structural order.

The exact location of the Si-N band is directly related to the N-H bond concentration. A higher N-H concentration results in a shift of the band to higher wavenumbers, due to the different electronegativities of Si and H.

Finally, the refractive index measurements are consistent with the Si content and the density of the film. Higher values of the Si content and the density of the film produce higher refractive index values.

ACKNOWLEDGMENTS

The authors would like to thank EPSRC, BP Solar, and South Bank University for support. Thanks are also due to Dr N. P. Barradas and Dr C. Jaynes of Surrey University Ion Beam Facility for the RBS and ERDA measurements. LOT-Oriel are thanked for the ellipsometry measurements We also acknowledge C.A.I de Espectroscopía (UCM, Spain) for availability of the FTIR spectrometer and CICYT (Spain) for partial financing under contract TIC2001/1253.

REFERENCES

- [1] Cai L, Rohatgi A, Han S, May G and Zou M 1998 *J. Appl. Phys.* **83** 5885.
- [2] Lauinger T, Schmidt J, Aberle A G and Hezel R 1996 *Appl. Phys. Lett.* **68** 1232.
- [3] Demichelis F, Crovini G, Giorgis F, Pirri C F and Tresso E 1996 *J. Appl. Phys.* **79** 1730.

- [4] Dzioba S and Rousina R 1994 *J. Vac. Sci. Technol. B* **12** 433.
- [5] Stryahilev D, Sazonov A and Nathan A 2002 *J. Vac. Sci. Technol. A* **20** 1087.
- [6] Knipp D, Street R A, Völkel A and Ho J 2003 *J. Appl. Phys.* **93** 347.
- [7] Peláez R, Castán E, Dueñas S, Barbolla J, Redondo E, Mártil I and González-Díaz G 1999 *J. Appl. Phys.* **86** 6924.
- [8] Hugon M C, Delmotte F, Agius B, and Courant J L 1997 *J. Vac. Sci. Technol. A* **15** 3143.
- [9] Kessels W M M, Hong J, van Assche F J H, Moschner J D, Lauinger T, Soppe W J, Weeber A W, Schram D C and van de Sanden M C M 2002 *J. Vac. Sci. Technol. A* **20** 1704.
- [10] Rohatgi A and Jeong J W 2003 *Appl. Phys. Lett.* **82** 224.
- [11] Ohta H, Hori M and Goto T 2001 *J. Appl. Phys.* **90** 1955.
- [12] Doughty C, Knick D C, Bailey J B and Spencer J E 1999 *J. Vac. Sci. Technol. A* **17** 2612.
- [13] Lee J W, Mackenzie K D, Johnson D, Shul R J, Hahn Y B, Hays D C, Abernathy C R, Ren F and Pearton S J 1999 *J. Vac. Sci. Technol. A* **17** 2183.
- [14] Lapeyrade M, Besland M P, Meva'a C, Sibäi A and Hollinger G 1999 *J. Vac. Sci. Technol. A* **17** 433.
- [15] Delmotte F, Hugon M C, Agius B and Courant J L 1997 *J. Vac. Sci. Technol. B* **15** 1919.
- [16] Hugon M C, Delmotte F, Agius B and Courant J L 1997 *J. Vac. Sci. Technol. A* **15**, 3143.
- [17] Ye C, Ning Z, Shen M, Cheng S and Gan Z 1998 *J. Appl. Phys.* **83** 5978.
- [18] Martínez F L, San Andrés E, del Prado A, Mártil I, Bravo D and López F J 2001 *J. Appl. Phys.* **90** 1573.
- [19] Martínez F L, del Prado A, Mártil I, González-Díaz G, Bohne W, Fuhs W, Röhrich J, Selle B and Sieber I 2001 *Phys. Rev. B* **63** 245320.
- [20] Martínez F L, del Prado A, Mártil I, Bravo D and López F J 2000 *J. Appl. Phys.* **88** 2149.
- [21] Martínez F L, del Prado A, Mártil I, González-Díaz G, Kliefoth K and Füssel W 2001 *Semicond. Sci. Technol.* **16** 534.
- [22] Redondo E, Blanco N, Mártil I and Gonzalez-Díaz G 1999 *Appl. Phys. Lett.* **74** 991.
- [23] Redondo E, Blanco N, Mártil I, González-Díaz G, Pelaez R, Dueñas S and Castán H 1999 *J. Vac. Sci. Technol. A* **17** 2178.
- [24] Redondo E, Mártil I, González-Díaz G, Castán H and Dueñas S 2001 *J. Vac. Sci. Technol. B* **19** 186.
- [25] Summers S, Reehal H S and Shirkoohi G H 2001 *J. Phys. D* **34** 2782.

- [26] Azzam R M A and Bashara N M 1983 *Ellipsometry and Polarized Light* (New York: North-Holland Publishing).
- [27] Barradas N P, Jeynes C and Webb R P 1997 *Appl. Phys. Lett.* **71** 291.
- [28] Lanford W A and Rand M J 1978 *J. Appl. Phys.* **49** 2473.
- [29] Park D G, Tao M, Li D, Botchkarev A E, Fan Z, Wang Z, Mohammad S N, Rockett A, Abelson J R, Morkoc H, Heyd A R and Alterovitz S A 1996 *J. Vac. Sci. Technol. B* **14** 2674.
- [30] Sitbon S, Hugon M C, Agius B, Abel F, Courant J L and Puech M 1995 *J. Vac. Sci. Technol. A* **13** 2900.
- [31] Flemish J R and Pfeffer R L 1993 *J. Appl. Phys.* **74** 3277.
- [32] Kotecki D E and Chapple-Sokol J D 1995 *J. Appl. Phys.* **77** 1284.
- [33] Martínez F L, del Prado A, Bravo D, López F, Mártil I and González-Díaz G 1999 *J. Vac. Sci. Technol. A* **17** 1280.
- [34] Budhani R C, Bunshah R F and Flinn P A 1988 *Appl. Phys. Lett.* **52** 284.
- [35] He L N, Inokuma T and Hasegawa S 1996 *Jpn. J. Appl. Phys.* **35** 1503.
- [36] Sassella A 1993 *Phys. Rev. B* **48** 14208.
- [37] Richard P D, Markunas R J, Lucovsky G, Fountain G G, Mansour A N and Tsu D V 1985 *J. Vac. Sci. Technol. A* **3** 867.
- [38] García S, Martín J M, Mártil I, Fernández M, Iborra E and González-Díaz G 1995 *J. Non-Cryst. Solids* **187** 329.
- [39] Martínez F L, Mártil I, González-Díaz G, Selle B and Sieber I 1998 *J. Non-Cryst. Solids* **227-230** 523.
- [40] Smith D L 1993 *J. Vac. Sci. Technol. A* **11** 1843.
- [41] Bulkin P V, Swart P L and Lacquet B M 1994 *Thin Solid Films* **241** 247.
- [42] García S, Martín J M, Mártil I, Fernández M and González-Díaz G 1998 *Thin Solid Films* **317** 116.
- [43] Barbour J C and Stein H J 1992 *Mat. Res. Soc. Symp. Proc.* **235**, 775.
- [44] Tsu D V, Lucovsky G and Mantini M J 1986 *Phys. Rev. B* **33** 7069.
- [45] Budhani R C, Prakash S, Doerr H J and Bunshah R F 1987 *J. Vac. Sci. Technol. A* **5** 1644.
- [46] Landheer D, Rajesh K, Masson D, Hulse J E, Sproule G I and Quance T 1998 *J. Vac. Sci. Technol. A* **16** 2931.
- [47] Dzioba S, Meikle S and Streater R W 1987 *J. Electrochem. Soc.* **134** 2599.

- [48] Hattangady S V, Fountain G G, Rudder R A and Markunas R J 1989 *J. Vac. Sci. Technol. A* **7** 570.
- [49] Yin Z and Smith F W 1991 *Phys. Rev. B* **43** 4507.
- [50] Sassella A, Borghesi A, Corni F, Monelli A, Ottaviani G, Tonini R, Pivac B, Bacchetta M and Zanotti L 1997 *J. Vac. Sci. Technol. A* **15** 377.

FIGURE CAPTIONS

- Figure 1. Growth rate as a function of deposition temperature for samples deposited at 500 W and gas flow ratio $N_2/SiH_4=12.5$. The line is a guide for the eye.
- Figure 2. Non bonded H content as a function of gas flow ratio (N_2/SiH_4) for samples deposited at 230 °C (squares) and 310 °C (triangles). Lines are guides for the eye. Representative error bars are included.
- Figure 3. N-H and Si-H bond concentration as a function of the N_2/SiH_4 gas flow ratio for two deposition temperatures. As indicated by the arrows, closed symbols are used for the N-H concentration while open symbols are used for Si-H. Squares correspond to the sample series deposited at 230 °C and triangles to the series with a deposition temperature of 470 °C. Lines are drawn as guides for the eye. Error bars are an estimate of 10 % in the error of FTIR band calculations.
- Figure 4. Si-N stretching band wavenumber as a function of the N_2/SiH_4 ratio for three different deposition temperatures. Lines are a guide for the eye.
- Figure 5. FWHM of the Si-N stretching band as a function of the deposition temperature for the following gas flow ratios: $N_2(\text{sccm})/SiH_4(\text{sccm}) = 50/2$ (squares), $50/3$ (circles), $50/4$ (triangles), and $50/5$ (diamonds). Lines are guides for the eye.
- Figure 6. Refractive index at a wavelength of 633 nm as a function of the N_2/SiH_4 ratio for a series deposited at 310 °C. The line is guide for the eye.
- Figure 7. Refractive index versus wavelength for three deposition temperatures.
- Figure 8. The measured ion density at different nitrogen to silane gas ratios. The line is a linear fit.
- Figure 9. Wavenumber of the Si-N stretching band as a function of the N-H bond concentration. The line is a linear fit of the data points.

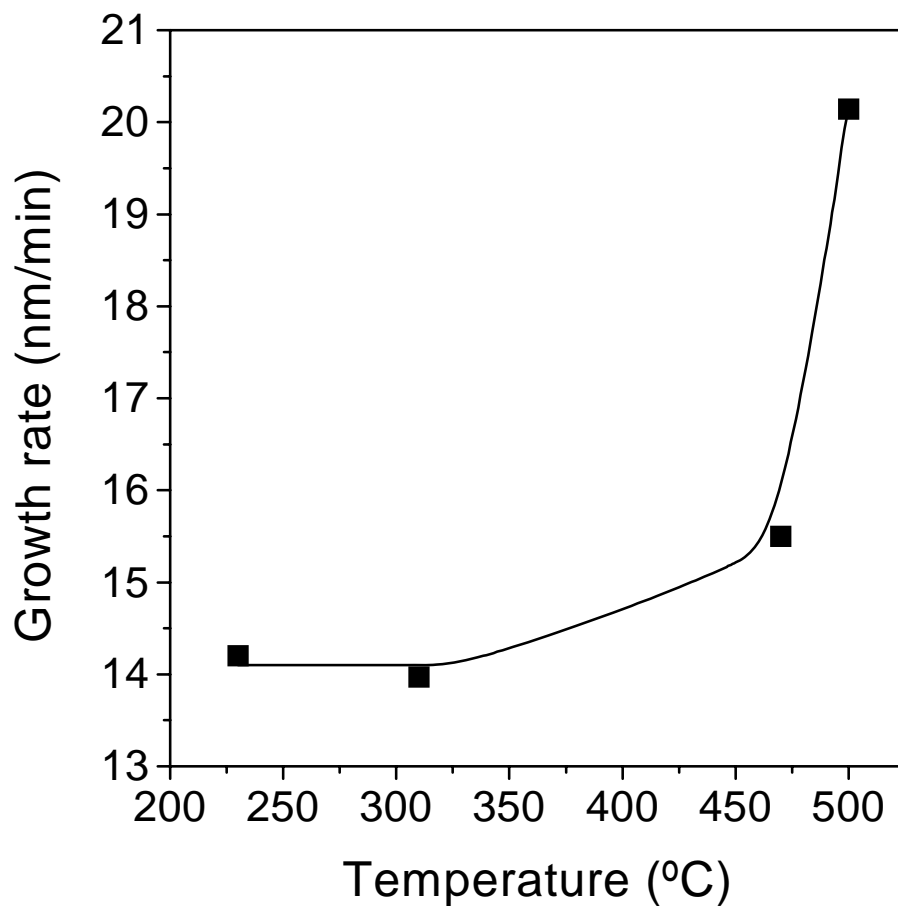


Figure 1

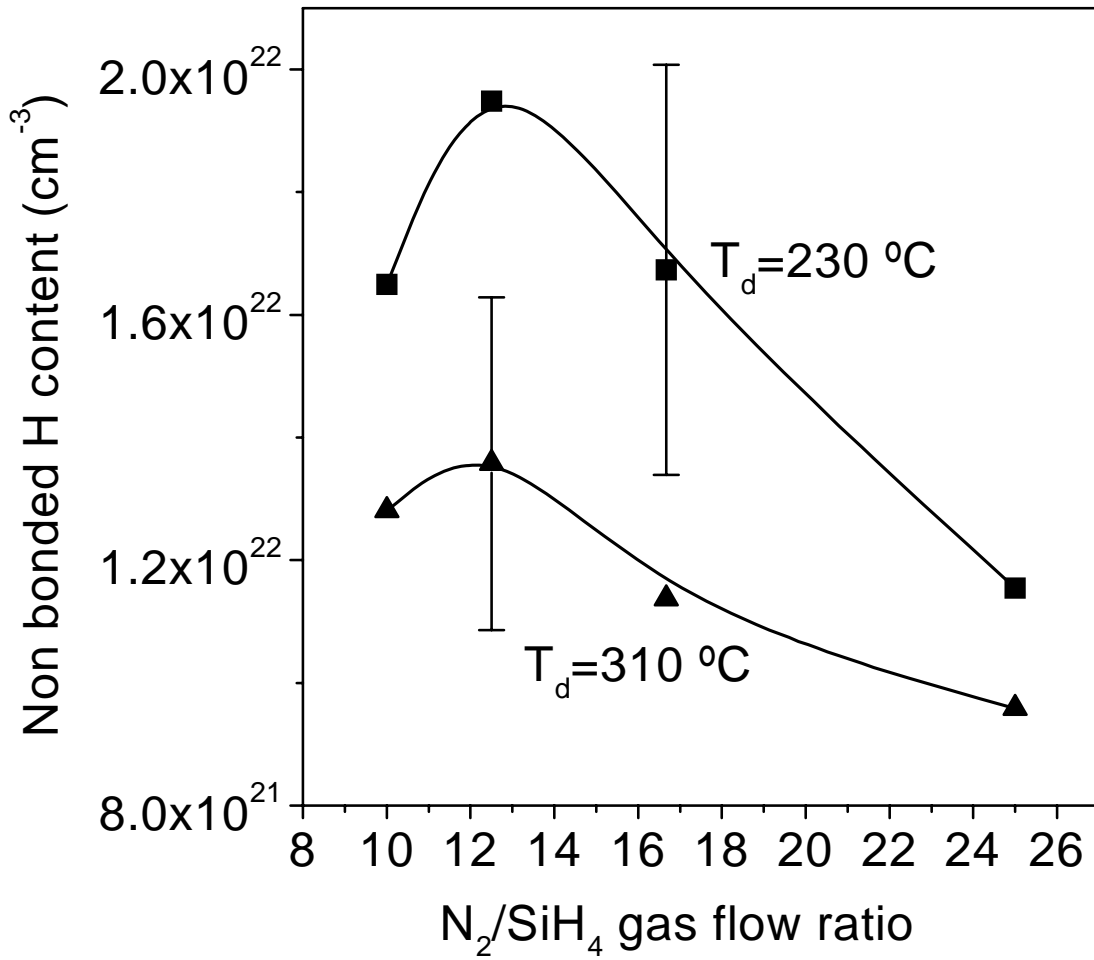


Figure 2

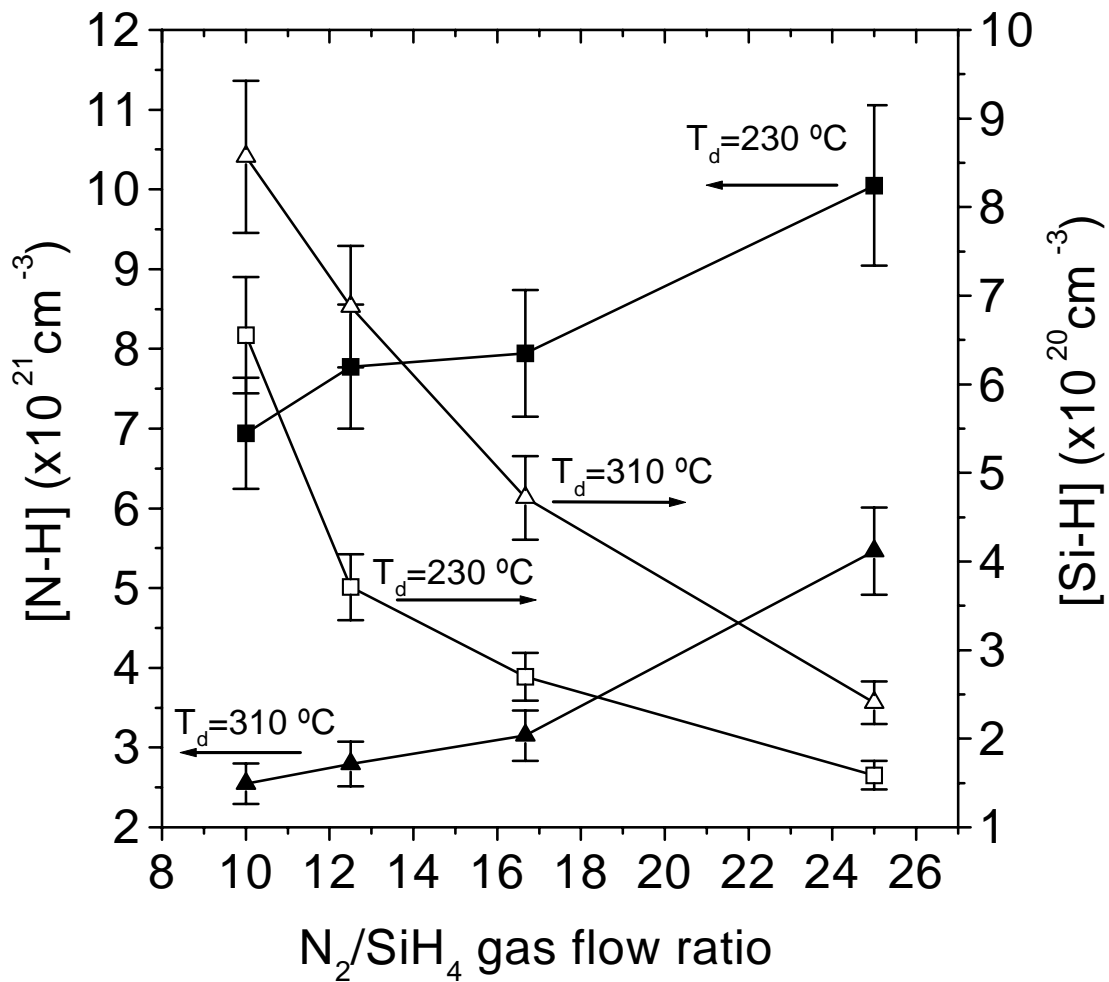


Figure 3

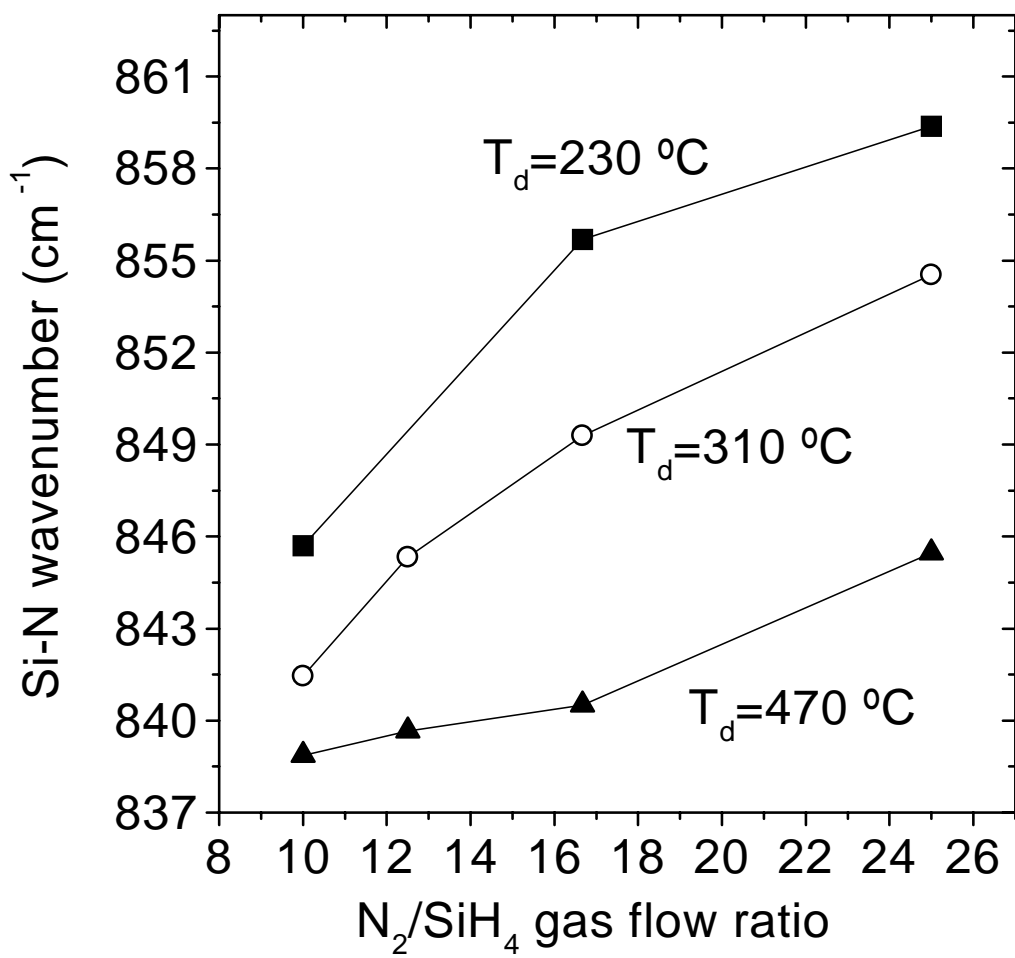


Figure 4

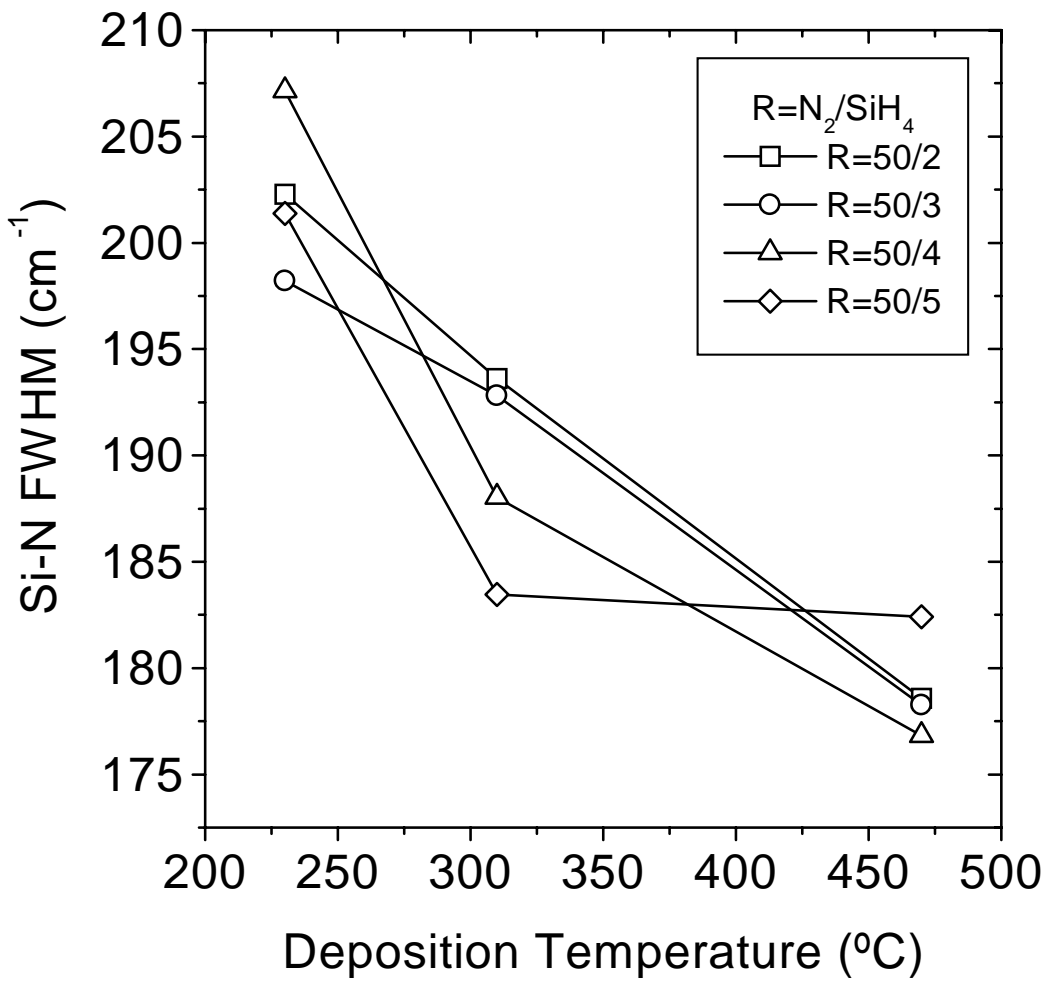


Figure 5

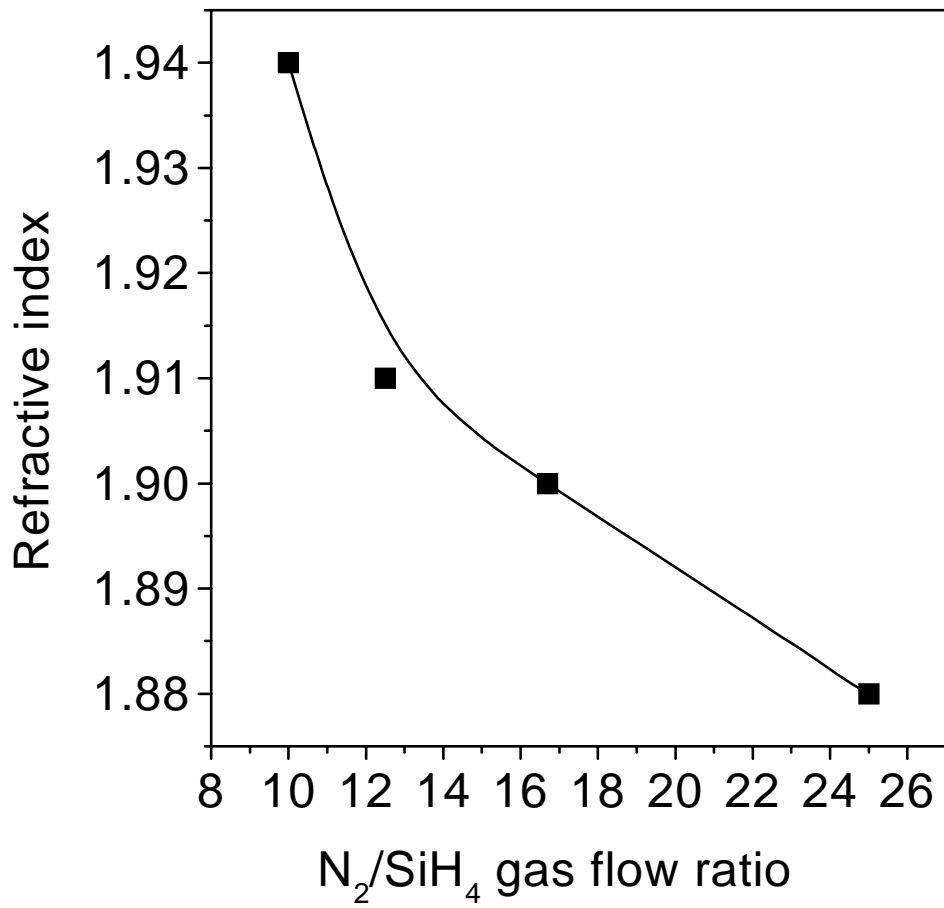


Figure 6

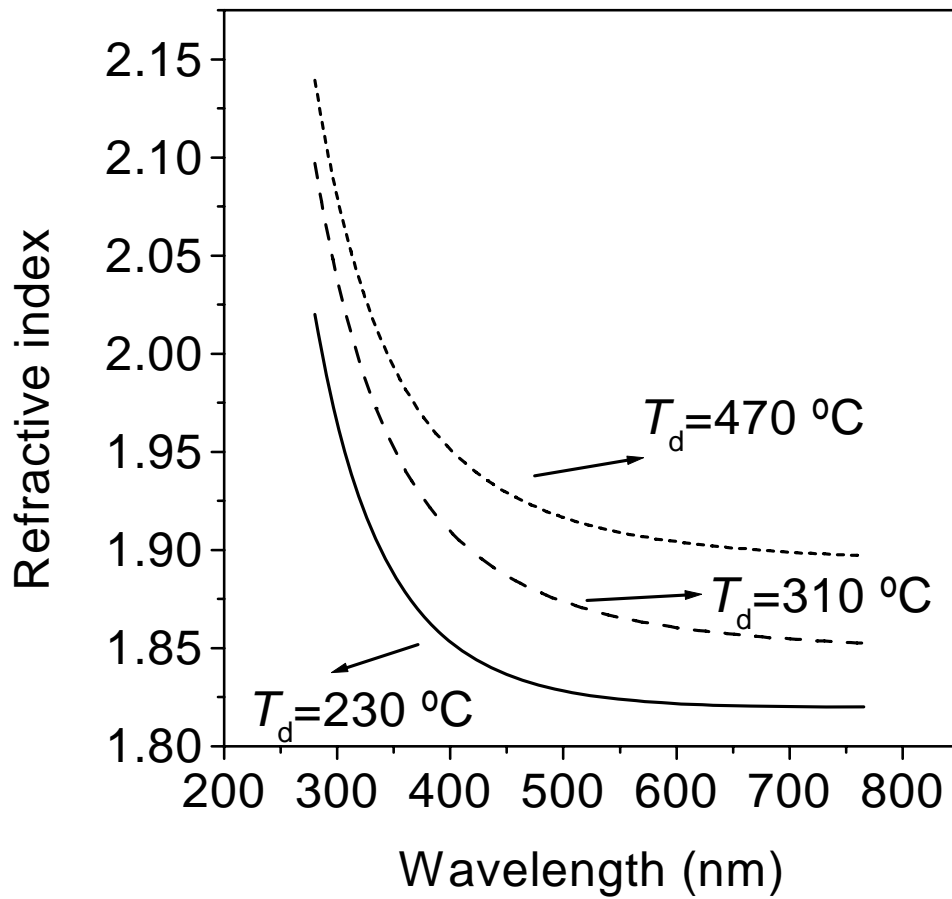


Figure 7

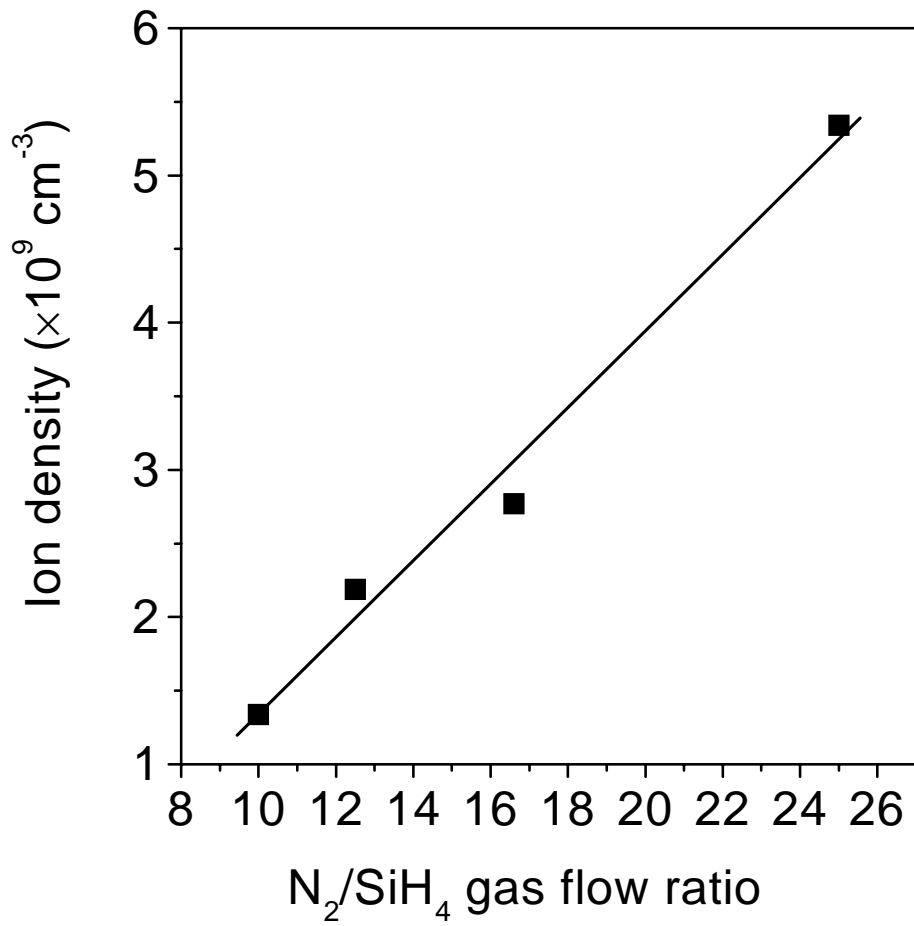


Figure 8

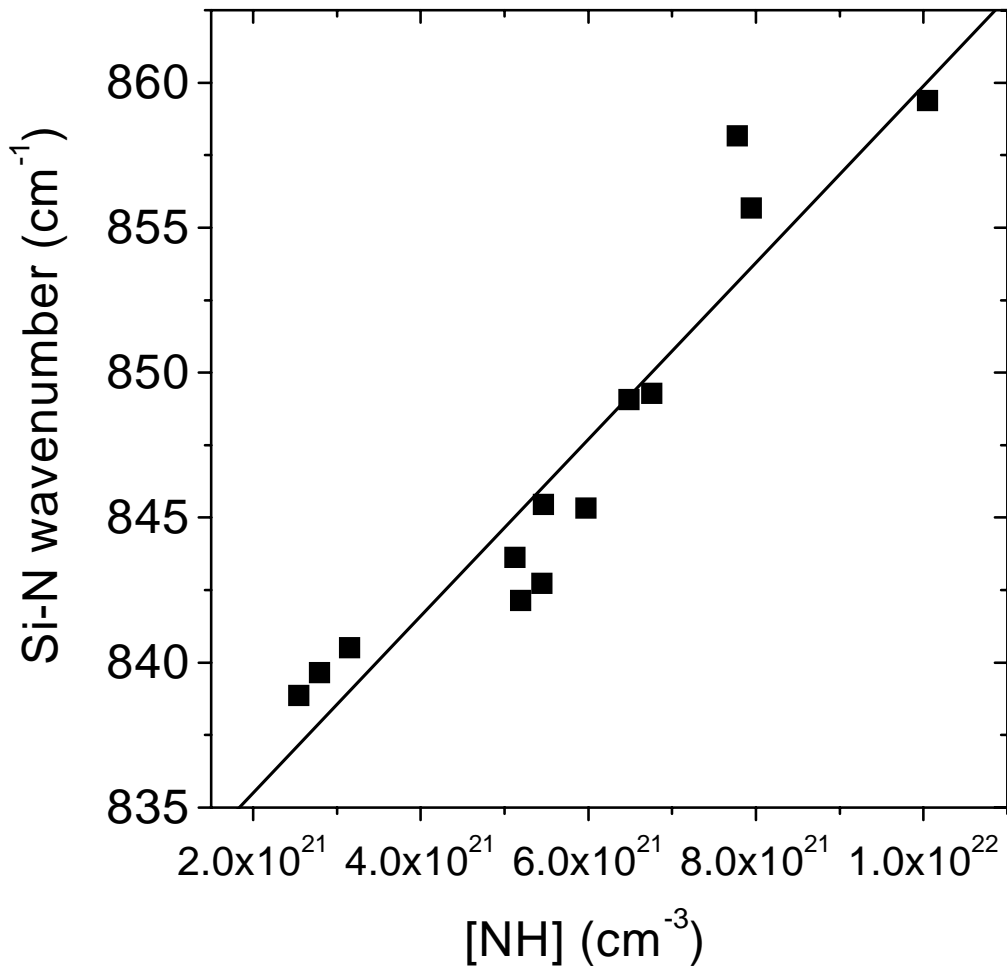


Figure 9

Table 1. Deposition parameters and results of the characterization by RBS (nitrogen and silicon content), ERDA (hydrogen content), and FTIR (density of bonded hydrogen).

Sample	Deposition Parameters			RBS/ERDA (Concentration)			RBS/ERDA (Atomic %)				FTIR Results	
	N ₂ :SiH ₄ (sccm)	Microwave power (W)	Temperature (°C)	[H] (10 ²² cm ⁻³)	[N] (10 ²² cm ⁻³)	[Si] (10 ²² cm ⁻³)	H (at%)	N (at%)	Si (at%)	N/Si ratio	[N-H] (10 ²¹ cm ⁻³)	[Si-H] (10 ²⁰ cm ⁻³)
aaa	50:2	200	230	2.2	4.5	2.9	22.6	47.0	30.4	1.6	10.0	1.6
aab	50:3	200	230	2.5	3.2	2.2	31.7	40.7	27.6	1.5	7.9	2.7
aac	50:4	200	230	2.8	4.1	3.1	27.7	41.3	31.0	1.3	7.8	3.7
aad	50:5	200	230	2.4	3.9	2.5	27.4	44.7	28.0	1.6	6.9	6.6
baa	50:2	200	310	1.5	2.9	1.8	24.7	46.4	28.9	1.6	5.6	1.6
bab	50:3	200	310	1.8	3.6	2.6	23.0	44.7	32.3	1.4	6.8	3.5
bac	50:4	200	310	2.0	4.3	2.8	22.0	47.0	31.0	1.5	6.0	3.8
bad	50:5	200	310	1.9	4.6	3.9	18.4	43.9	37.7	1.2	5.4	8.7
caa	50:2	200	470	2.0	3.8	2.8	23.4	44.3	32.3	1.4	5.5	2.4
cab	50:3	200	470	1.2	3.6	2.4	16.4	50.3	33.3	1.5	3.2	4.7
cac	50:4	200	470	1.2	5.7	4.4	10.3	50.9	38.8	1.3	2.8	6.8
cad	50:5	200	470	1.5	4.5	3.5	15.8	47.4	36.7	1.3	2.5	8.6
cac	50:4	200	470	1.2	5.7	4.4	10.3	50.9	38.8	1.3	2.8	6.8
cbc	50:4	300	470	1.3	4.2	2.5	16.7	51.9	31.3	1.7	5.1	4.9
ccc	50:4	400	470	1.3	4.8	4.0	12.9	47.1	40.0	1.2	5.4	3.9
cdc	50:4	500	470	1.6	4.5	3.6	16.6	46.3	37.1	1.3	6.5	1.9